

Vision–Motion–Reference Alignment for Referring Multi-Object Tracking via Multi-Modal Large Language Models

Weiye Lv¹ Ning Zhang² Hanyang Sun¹ Haoran Jiang¹ Kai Zhao³ Jing Xiao⁴ Dan Zeng^{1†}

^{1,3}Shanghai University ^{2,4}PAII Inc.

¹{kroery, sunhanyang, jianghaoran, dzeng}@shu.edu.cn

²ning.zhang@gmail.com ³kz@kaizhao.net ⁴xiaojing661@pingan.com.cn

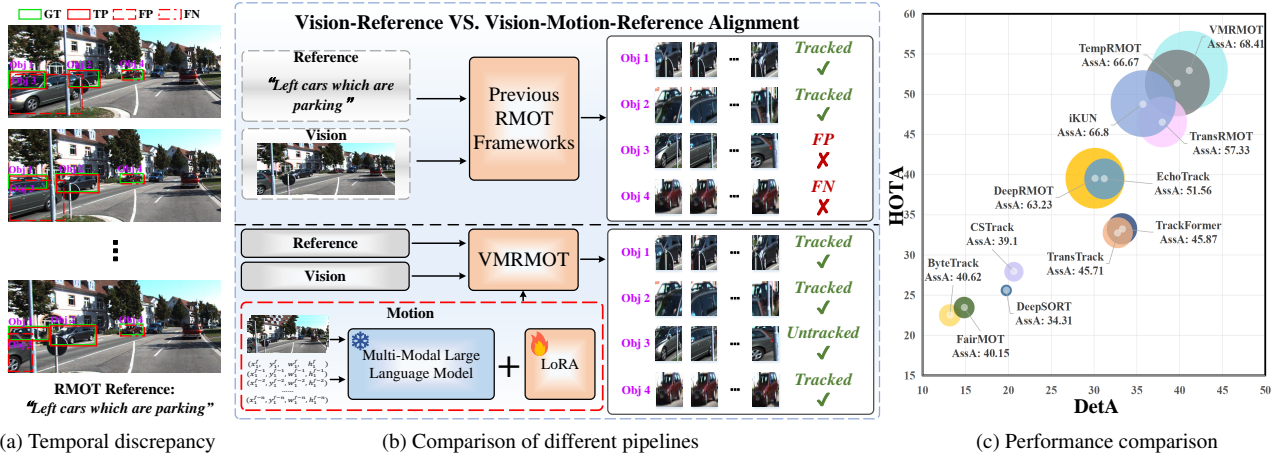


Figure 1. (a) illustrates the temporal discrepancy between the static reference “left cars which are parking” and the dynamic vision modality of objects 3 and 4, which leads to FP and FN. (b) shows the comparison between previous RMOT frameworks, which integrate only the vision and reference modalities, and our proposed VMRMOT, which incorporates vision, motion, and reference modalities. (c) shows the HOTA-DetA-AssA comparisons of different RMOT trackers on the Refer-KITTI dataset. Our VMRMOT achieves 53.00% HOTA, 41.13% DetA, and 68.41% AssA.

Abstract

Referring Multi-Object Tracking (RMOT) extends conventional multi-object tracking (MOT) by introducing natural language references for multi-modal fusion tracking. RMOT benchmarks only describe the object’s appearance, relative positions, and initial motion states. This so-called static regulation fails to capture dynamic changes of the object motion, including velocity changes and motion direction shifts. This limitation not only causes a temporal discrepancy between static references and dynamic vision modality but also constrains multi-modal tracking performance. To address this limitation, we propose a novel Vision–Motion–Reference aligned RMOT framework, named VMRMOT. It integrates a motion modality extracted from object dynamics to enhance the alignment between vision modality and language references through multi-modal large language models (MLLMs). Specifically, we introduce motion-aware descriptions derived from object dynamic behaviors and, leveraging the powerful

temporal-reasoning capabilities of MLLMs, extract motion features as the motion modality. We further design a Vision–Motion–Reference Alignment (VMRA) module to hierarchically align visual queries with motion and reference cues, enhancing their cross-modal consistency. In addition, a Motion-Guided Prediction Head (MGPH) is developed to explore motion modality to enhance the performance of the prediction head. To the best of our knowledge, VMRMOT is the first approach to employ MLLMs in the RMOT task for vision–reference alignment. Extensive experiments on multiple RMOT benchmarks demonstrate that VMRMOT outperforms existing state-of-the-art methods. The code is available at <https://github.com/Kroery/VMRMOT>.

1. Introduction

Referring Multi-Object Tracking (RMOT) is a recent active research branch of conventional multi-object tracking (MOT) [7, 8, 27, 28, 44], which introduces natural language

[†] Corresponding author.

references as an additional modality to specify the objects of interest (e.g., “Track left vehicles which are parking”). Unlike traditional MOT that relies only on visual appearance and motion cues, RMOT enables human-centered and instruction-driven tracking, bridging perception with natural communication. Benefiting from the integration of vision and reference modalities, RMOT has attracted increasing attention in various applications such as video editing [13], autonomous driving [22, 47], and animal surveys [12].

Existing RMOT methods [6, 36, 46] encode the features of language references and fuse them directly with visual representations, either at early feature extraction stages or using them later to select tracking results. However, current RMOT benchmarks formulate language references through static regulations, which are manually defined rules or templates that describe objects without considering their temporal dynamics. Such static references typically encode static attributes (e.g., color, category, or relative position) or initial motion states (e.g., initial velocity or starting location). On the other hand, the vision modality encompasses the evolving behaviors of objects over time, including changes in velocity, (de/ac)celeration, and abrupt motion direction changes. Since static references cannot fully represent such temporal dynamics, existing methods fail to achieve accurate cross-modal alignment. This is due to their exclusive dependency on static references. As illustrated in Fig. 1 (a), the temporal discrepancy between static references and the vision modality often results in false positives (FP) and false negatives (FN), thereby limiting the effectiveness of multi-modal tracking.

Recognizing the importance of aligning static references with the vision modality, some efforts [16, 18, 20] have begun to explore the decoupling of language references into finer-grained components. Despite these advances, such methods still rely on static references. Consequently, they do not account for the dynamic changes in object behavior observed across video sequences, limiting their ability to achieve precise vision–reference temporal alignment.

In this paper, we propose a novel Vision–Motion–Reference aligned RMOT framework named VMRMOT. It aims to bridge the discrepancy between static language references and the vision modality. As shown in Fig. 1 (b), different from previous RMOT frameworks, VMRMOT leverages MLLMs to introduce a motion modality to facilitate vision–reference alignment. Specifically, we first generate motion-aware descriptions that explicitly encode the dynamic behaviors of objects. From each object’s historical trajectory, we extract key motion cues including position, motion direction, distance trend, and speed trend, and organize them into compact natural-language descriptions. These motion descriptions effectively compress historical motion into a compact textual representation, capturing temporal dynamics that

static references cannot. Then, we leverage the temporal reasoning and cross-modal alignment capabilities of MLLMs to extract motion features as the motion modality. To hierarchically fuse motion and reference modalities into the vision modality, we design a Vision–Motion–Reference Alignment (VMRA) module that sequentially integrates motion and reference cues into visual queries. This hierarchical fusion allows the model to first incorporate temporal motion cues, then refine alignment with static language semantics, ensuring robust multi-modal tracking. Furthermore, we introduce a Motion-Guided Prediction Head (MGPH), which leverages motion modality to enhance the performance of the prediction head.

To the best of our knowledge, VMRMOT is the first work to introduce MLLMs into RMOT for explicit vision–reference alignment. Extensive experiments on multiple RMOT benchmarks demonstrate that our method consistently outperforms state-of-the-art approaches. As we can see in Fig. 1 (c), VMRMOT achieves the best overall performance in terms of HOTA, DetA, and AssA metrics on the Refer-KITTI dataset. The results confirm that introducing the motion modality effectively enhances the alignment between reference and vision modalities, leading to improved cross-modal tracking performance.

In summary, our contribution is three-fold:

- We propose a novel RMOT framework, VMRMOT, which incorporates a motion modality via MLLMs to enhance vision–language alignment.
- We design a VMRA module and an MGPH. The VMRA leverages motion cues to enhance the alignment between vision and reference features, while the MGPH leverages motion modality to enhance the performance of the prediction head.
- VMRMOT outperforms SOTA methods on multiple public RMOT benchmarks, consistently improving HOTA, DetA, and AssA metrics.

2. Related Work

Referring Multi-Object Tracking. Recently, referring understanding [4, 14, 15, 17, 21, 32, 37, 38, 45, 49] has attracted great attention, benefiting from its flexibility and alignment with human intentions. As an emerging referring understanding task, RMOT has advanced rapidly since the first baseline model TransRMOT [36] is introduced. TransRMOT is built upon the end-to-end multi-object tracking method MOTR [42] by adding an early visual-reference fusion module. iKUN [6] follows a two-stage RMOT paradigm. It first extracts object tracklets using an existing tracker, and then matches tracklets with references. TempRMOT [46] integrates temporal information into the model on top of TransRMOT. Other works [3, 10, 29, 39, 50] follow a similar approach, either integrating references with visual features at early stages or

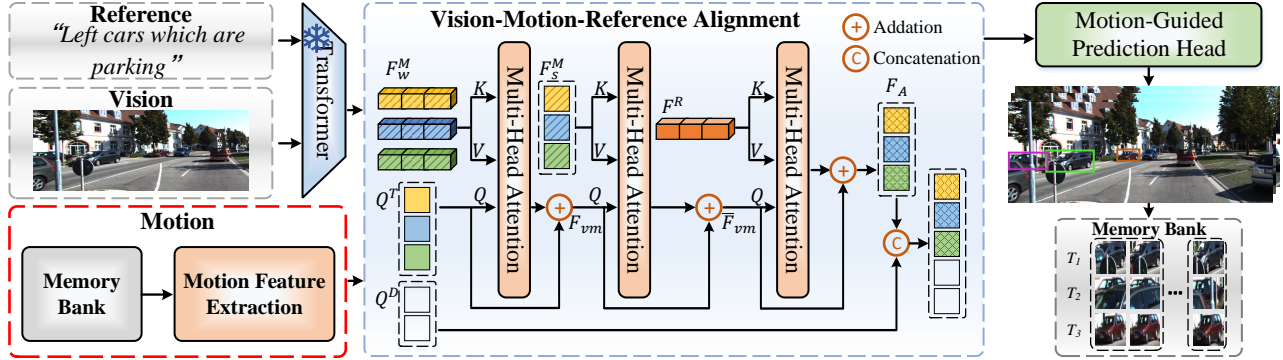


Figure 2. The overall architecture of VMRMOT. VMRMOT consists of four parts: a frozen transformer, a motion feature extraction, a vision–motion–reference alignment, and a motion-guided prediction head.

using them later to filter tracking results. However, these approaches do not fully exploit the fine-grained reference cues.

Recognizing that different linguistic cues can play distinct roles at different tracking stages, some efforts [16, 18, 20] begin to explore the decoupling of language references. DKGTrack [16] decouples language references into localized descriptions and motion states for precise object tracking. CDRMT [20] emulates the “what” and “where” pathways from the human visual processing system to cognitively decouple references. However, these methods still rely on decoupling within references. Such references, formulated through static regulations, primarily describe the objects’ static attributes or initial motion states, making them difficult to align with dynamic vision modality. In this paper, we explicitly extract motion modality from the dynamic behaviors of objects to facilitate alignment between the vision modality and static references.

MLLMs in Video Referring Understanding. Leveraging the strong reasoning and cross-modal capabilities, MLLMs have recently been applied to Video Referring Understanding tasks [2, 5, 33, 41, 48]. TrackGPT [33] made the first attempt to leverage MLLMs for reasoning-based object segmentation in videos. VISA [41] leverages MLLMs to perform reasoning-based video object segmentation, generating mask sequences from implicit text queries while incorporating world knowledge and temporal context. ReferGPT [2] introduces a zero-shot RMOT framework that employs MLLMs to generate object descriptions for reference matching. In contrast, VMRMOT leverages MLLMs to extract motion features as a motion modality to enhance visual–reference alignment.

3. Method

3.1. Framework Overview

In this section, we introduce VMRMOT, a novel framework that achieves vision–motion–reference alignment for

RMOT. As illustrated in Fig. 2, VMRMOT follows the end-to-end transformer-based tracking architecture [42], and consists of four main components: a frozen transformer, a motion feature extraction, a vision–motion–reference alignment, and a motion-guided prediction head.

Transformer. Given a video sequence V and a natural language reference \mathcal{E}^R . VMRMOT adopts a transformer-based tracker following the design of TransRMOT [36]. A ResNet-50 backbone is employed to extract the visual features from each input frame, while a pre-trained RoBERTa model [25] encodes the references to obtain reference embeddings $F^R \in \mathbb{R}^{L^R \times D}$, where L^R refers to the length of reference words and D refers to the feature dimension. An early-fusion module integrates the reference and visual features, allowing the tracker to inject reference semantics into the visual features at an early stage. The fused features are then fed into a stack of deformable transformer encoder and decoder layers, which perform cross-modal interaction and temporal reasoning to associate objects across frames. Finally, the transformer outputs a set of detection queries Q^D and track queries Q^T , which incorporate preliminary reference information. These queries serve as the initial representations for object localization and identity association.

Motion Feature Extraction. For each track query, the historical trajectories stored in a memory bank \mathcal{M} are first retrieved and converted into motion-aware descriptions \mathcal{E}^M . These descriptions summarize the dynamic behaviors of objects, including position, motion direction, distance trends, and speed trends. The motion-aware descriptions and the previous n frames are jointly fed into MLLMs to obtain motion features as the motion modality, which capture object behaviors and their temporal consistency with visual sequences.

Vision–Motion–Reference Alignment. The motion features are integrated with the track queries and reference features within the VMRA module. The track queries hierarchically align with motion and reference cues and yield motion- and reference-enhanced visual representations.

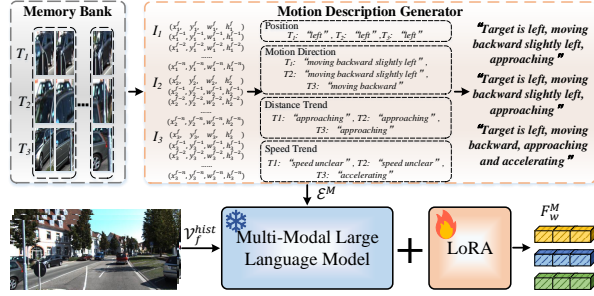


Figure 3. Illustration of the Motion feature extraction pipeline. It consists of two stages: first, historical trajectories are converted into compact motion-aware descriptions; then, MLLMs are employed to extract motion features from these descriptions.

Motion-Guided Prediction Head. The MGPB leverages the motion modality to refine both the box and the referring branches, enhancing the accuracy and consistency of the predicted trajectories. The predicted object states are then updated in the memory bank \mathcal{M} to provide historical motion information for subsequent tracking.

The detailed motion feature extraction process is described in Sec. 3.2, and the designs of VMRA and MGPB are presented in Sec. 3.3 and Sec. 3.4, respectively.

3.2. Motion Feature Extraction via MLLMs

The purpose of the Motion feature extraction is to obtain motion features from the historical trajectories of tracked objects, which are utilized as the motion modality in the proposed framework. The pipeline is illustrated in Fig. 3. First, historical trajectories are converted into compact motion-aware descriptions that capture the semantic evolution of object movements. Then, leveraging the reasoning and alignment capabilities of MLLMs, the motion descriptions are transformed into motion features that encode rich temporal information and provide a structured embedding of object dynamics.

Motion-aware Description Generation. To comprehensively characterize the dynamic behaviors of tracked objects, we describe their temporal evolution from four complementary aspects: position, motion direction, distance trend, and speed trend. These aspects jointly capture both spatial and temporal variations — where the position reflects the object’s relative location, the motion direction indicates its movement orientation, the distance trend reveals its approach or departure from the camera, and the speed trend describes the acceleration or deceleration patterns.

For each tracked object T_i , we first retrieve its historical trajectory from the memory bank. Let $I = \{B_{f-n}, B_{f-n+1}, \dots, B_f\}$ denote the historical motion information of a tracked object, where f is the frame index, and $B_f = (x_f, y_f, w_f, h_f)$ is the object’s bounding box representing the coordinates of the center point and the

height and width of the box. The historical motion information I is thus defined as the sequence of bounding boxes from the previous n frames, which encapsulates the object’s recent spatial and scale variations.

Based on I , we compute four motion descriptors to describe the object’s dynamic behaviors. The **position** descriptor is determined by the normalized center coordinates of the bounding box:

$$P_f = \left(\frac{x_f}{W}, \frac{y_f}{H} \right), \quad (1)$$

where W and H denote the frame width and height, respectively. The position descriptor is then converted into a textual phrase $\langle \text{position} \rangle$, such as “ahead”, “left”, or “right”. The **motion direction** descriptor is computed from the displacement between consecutive frames:

$$\Delta x_f = x_f - x_{f-1}, \quad \Delta y_f = y_f - y_{f-1}, \quad (2)$$

and is converted into a textual phrase $\langle \text{motion direction} \rangle$, such as “moving forward”, or “moving backward”. The **distance trend** descriptor captures changes in the object’s scale:

$$A_f = w_f \cdot h_f, \quad \Delta A_f = A_f - A_{f-1}, \quad (3)$$

The distance trend is then expressed as a textual phrase $\langle \text{distance trend} \rangle$, such as “approaching”, “moving away”, or “staying at distance”. The **speed trend** descriptor is derived from the change in speed magnitude:

$$v_f = \sqrt{(\Delta x_f)^2 + (\Delta y_f)^2}, \quad \Delta v_f = v_f - v_{f-1}, \quad (4)$$

and is converted into a textual phrase $\langle \text{speed trend} \rangle$, such as “accelerating”, “decelerating”, or “constant speed”.

Finally, the four descriptors are combined to form the motion-aware description. The motion description \mathcal{E}^M follows the template:

$$\text{Target is } \langle \text{position} \rangle, \langle \text{motion direction} \rangle, \langle \text{distance trend} \rangle \\ \text{[and } \langle \text{speed trend} \rangle].$$

Motion Feature Extraction. To obtain motion features as the motion modality, we leverage MLLMs to transform motion descriptions into representations that capture temporal dynamics and semantic correlations with visual sequences. Specifically, for each tracked object at frame f , the motion-aware description \mathcal{E}^M consisting of L^M words and the visual sequence consisting of the previous n frames $\mathcal{V}_f^{\text{hist}} = \{\mathbf{F}_{f-n}^{\text{vis}}, \mathbf{F}_{f-n+1}^{\text{vis}}, \dots, \mathbf{F}_f^{\text{vis}}\}$ where $\mathbf{F}_i^{\text{vis}}$ denotes the image of frame i , are fed into a multi-modal large language model $\text{MLLM}(\cdot)$:

$$F_w^M = \text{MLLM}(\mathcal{E}_f^M, \mathcal{V}_f^{\text{hist}}), \quad (5)$$

where $F_w^M \in \mathbb{R}^{L^M \times D}$ represents the word-level motion features output by the last layer of the MLLM, which can be

further average-pooled to obtain the sentence-level motion feature $F_s^M \in \mathbb{R}^{1 \times D}$. The MLLM is jointly trained with the overall VMRMOT framework and LoRA-finetuned specifically on the text encoding and multi-modal fusion modules to better process motion-aware descriptions, which differ from conventional natural language references.

3.3. Vision-Motion-Reference Alignment

As shown in Fig. 2, we design a VMRA module that hierarchically aligns visual queries with motion and reference embeddings to enhance cross-modal consistency. Given the visual track query Q^T , the sentence-level motion feature F_s^M , the word-level motion feature F_w^M , and the reference feature F^R , the VMRA module hierarchically fuses these features through multi-stage cross-attention to produce a unified embedding. We perform the VMRA exclusively on track queries, and detection queries are separated and remain unaffected during this process.

The VMRA first modulates the interaction between the visual query Q^T and the fine-grained motion semantics F_w^M , allowing the model to perceive detailed temporal variations such as "moving left", "accelerating", or "approaching". This process is formulated as:

$$\mathbf{F}_{vm} = \text{MHA}(Q^T, \mathbf{F}_w^M, \mathbf{F}_w^M) + Q^T, \quad (6)$$

where $\text{MHA}(\cdot)$ denotes multi-head attention. Through this step, the visual query dynamically aggregates fine-grained motion cues, enhancing temporal awareness.

Next, the vision-motion feature \mathbf{F}_{vm} interacts with the sentence-level motion embeddings F_s^M through another cross-attention layer:

$$\bar{\mathbf{F}}_{vm} = \text{MHA}(\mathbf{F}_{vm}, F_s^M, F_s^M) + \mathbf{F}_{vm}, \quad (7)$$

where the attention is computed across all tracked objects, allowing each query position to access the sentence-level motion summaries of other objects. This design enables global motion interactions that enhance consistency among correlated trajectories, thereby strengthening the coherence between local dynamics and overall motion semantics.

Finally, the vision-motion-enhanced feature $\bar{\mathbf{F}}_{vm}$ is aligned with the reference features F^R to ensure semantic consistency across modalities:

$$\mathbf{F}_A = \text{MHA}(\bar{\mathbf{F}}_{vm}, F^R, F^R) + \bar{\mathbf{F}}_{vm}. \quad (8)$$

The resulting multi-modal feature \mathbf{F}_A is then used to update the original track query Q^T , producing a motion- and reference-aware query that integrates vision, motion, and reference modalities. The updated track queries are then concatenated with the detection queries and fed into the MGPH. Through this hierarchical fusion, the VMRA module produces temporally coherent and semantically enriched features that serve as a robust foundation for the subsequent prediction head.

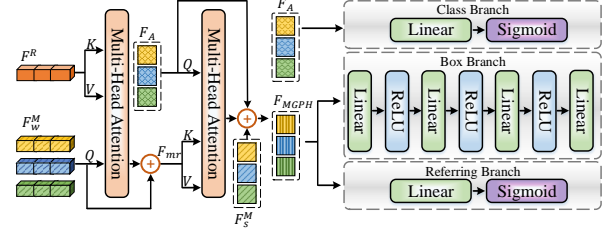


Figure 4. Illustration of MGPH, where motion and reference embeddings are fused to produce motion- and reference-aware features for prediction. MGPH consists of three branches: a class branch, a box branch, and a referring branch.

3.4. Motion-Guided Prediction Head

To accurately predict object states while leveraging both motion and reference cues, each query first passes through a Temporal Enhancement Module, following TempRMOT [46], to strengthen its temporal perception from historical frames. The temporally enhanced query is then fed into the MGPH, where motion- and reference-aware features are fused to produce motion- and reference-aware features for prediction.

In MGPH, the motion- and reference-aware features are fused with the updated track query \mathbf{F}_A through multi-head cross-attention operations. Specifically, the reference features F^R , along with the sentence-level and word-level motion features F_s^M and F_w^M , are integrated with the track query as follows.

First, the word-level motion features F_w^M are aligned with the reference features F^R through cross-attention, producing a motion-reference fused representation:

$$\mathbf{F}_{mr} = \text{MHA}(F_w^M, F^R, F^R) + F_w^M, \quad (9)$$

Next, the track query \mathbf{F}_A attends to the fused motion-reference feature \mathbf{F}_{mr} , integrating both motion and reference information while retaining the global motion context through a residual connection with the sentence-level motion embedding F_s^M . This design allows the query to simultaneously leverage local temporal cues, overall motion trends, and linguistic references, improving the accuracy and consistency of trajectory prediction. The final motion- and reference-aware feature is computed as

$$\mathbf{F}_{MGPH} = \text{Linear}(\text{MHA}(\mathbf{F}_A, \mathbf{F}_{mr}, \mathbf{F}_{mr}) + \mathbf{F}_A + F_s^M), \quad (10)$$

where Linear denotes a linear layer, and \mathbf{F}_{MGPH} is subsequently used for bounding box regression and reference confidence prediction.

Finally, the MGPH predicts the object class, reference alignment confidence, and bounding box offsets. The class branch applies a linear layer with a sigmoid activation to produce a confidence score, indicating whether a query represents a valid object. The referring branch similarly uses

Method	Detector	E	HOTA \uparrow	DetA \uparrow	AssA \uparrow	DetRe \uparrow	DetPr \uparrow	AssRe \uparrow	AssPr \uparrow	MOTA \uparrow	IDF1 \uparrow
FairMOT [43]	DLA-34	\times	23.46	14.84	40.15	17.40	43.58	53.35	73.15	0.80	26.18
DeepSORT [35]	DLA-34	\times	25.59	19.76	34.31	26.38	36.93	39.55	61.05	-	-
ByteTrack [44]	DLA-34	\times	22.49	13.17	40.62	16.13	36.61	46.09	73.39	-7.52	23.72
CSTrack [19]	YOLOv5	\times	27.91	20.65	39.10	33.76	32.61	43.12	71.82	-	-
TransTrack [34]	DeformableDETR	\times	32.77	23.31	45.71	32.33	42.23	49.99	79.48	-	-
TrackFormer [30]	DeformableDETR	\times	33.26	25.44	45.87	35.21	42.19	50.26	79.63	-	-
iKUN [6]	DeformableDETR	\times	48.84	35.74	66.80	51.97	52.25	72.95	87.09	12.26	54.05
EchoTrack [23]	DeformableDETR	\checkmark	39.47	31.19	51.56	42.65	48.86	56.68	81.21	-	-
DeepRMOT [10]	DeformableDETR	\checkmark	39.55	30.12	53.23	41.91	47.47	58.47	82.16	-	-
TransRMOT [36]	DeformableDETR	\checkmark	38.06	29.28	50.83	40.20	47.36	55.43	81.36	9.03	46.40
TransRMOT* [36]	DeformableDETR	\checkmark	46.56	37.97	57.33	49.69	60.10	60.02	89.67	17.88	53.60
TempRMOT \ddagger [46]	DeformableDETR	\checkmark	51.40	39.72	66.67	53.55	59.13	71.98	87.24	24.84	58.75
VMRMOT	DeformableDETR	\checkmark	53.00	41.13	68.41	55.63	59.74	73.28	88.61	26.66	61.06

Table 1. Comparison with state-of-the-art RMOT trackers on the Refer-KITTI test sets. * denotes the results after frame correction. \ddagger represents the results obtained by directly evaluating using the official open source code and weights. "E" means the End-to-End methods. \uparrow means the higher the better. **Bold** numbers indicate the best results.

Method	Detector	E	HOTA \uparrow	DetA \uparrow	AssA \uparrow	DetRe \uparrow	DetPr \uparrow	AssRe \uparrow	AssPr \uparrow
FairMOT [43]	DLA-34	\times	22.53	15.80	32.82	20.60	37.03	36.21	71.94
ByteTrack [44]	DLA-34	\times	24.59	16.78	36.63	22.60	36.18	41.00	69.63
iKUN [6]	DeformableDETR	\times	10.32	2.17	49.77	2.36	19.75	58.48	68.64
TransRMOT [36]	DeformableDETR	\checkmark	31.00	19.40	49.68	36.41	28.97	54.59	82.29
TempRMOT \ddagger [46]	DeformableDETR	\checkmark	34.05	22.22	52.50	32.58	40.20	58.17	81.65
VMRMOT	DeformableDETR	\checkmark	35.21	23.96	51.95	37.03	39.59	57.56	81.34

Table 2. Comparison with state-of-the-art RMOT trackers on the Refer-KITTI-V2 test sets. \ddagger represents the results obtained by directly evaluating using the official open source code and weights. "E" means the End-to-End methods.

a linear layer with sigmoid activation to evaluate the alignment between the query and the language reference. The box branch employs a compact multi-layer perceptron to predict bounding box offsets, which are then added to the prior box estimates to yield refined object positions. The resulting object states are subsequently stored in the memory bank \mathcal{M} to provide historical information for future frames.

4. Experiments

4.1. Experimental Setup

Datasets. We conducted the main experiments on Refer-KITTI [36] and Refer-KITTI-V2 [46] datasets. Refer-KITTI is the first publicly available dataset for RMOT, derived from the KITTI [9] benchmark with manually annotated referring expressions, which includes 15 training videos with 660 descriptions and 3 test videos with 158 annotations. Refer-KITTI-V2 is an extension of Refer-KITTI, expanding the dataset with the full KITTI sequences and replacing manual annotations with LLM-generated referring expressions, resulting in 17 training videos with 8,873 annotations and 4 test videos with 897 annotations.

Evaluation Metrics. We utilize Higher Order Metric

[26] (HOTA, DetA, AssA), IDF1 [31], and CLEAR metrics [1] (MOTA) as our main evaluation metrics. HOTA serves as the primary metric, balancing detection and association accuracy. IDF1 and AssA measure association performance, while DetA and MOTA mainly assess detection quality. Notably, in RMOT, an object is regarded as a true positive (TP) only when it correctly matches the reference description. Therefore, MOTA, which is heavily influenced by false positives (FP) and false negatives (FN), intuitively reflects the model’s ability to align visual objects with references.

Implementation Details. Our training process is conducted in two stages. First, we follow the training setup of TempRMOT [46] to pre-train the transformer for 60 epochs. Then, the transformer is frozen, and the entire framework, including VMRA, MGPH, and the MLLM components, is jointly fine-tuned. The MLLM module leverages LoRA [11] for efficient fine-tuning of the text encoder and cross-modal fusion layers. For optimization in the second stage, we adopt the AdamW optimizer with an initial learning rate of 10^{-5} , and fine-tune the model for 5 epochs, where the learning rate is decayed by a factor of 10 at the 4th epoch. The batch size is set to 1. All experiments are conducted on

Base	VMRA	MGPB	HOTA↑	DetA↑	AssA↑
✓			51.40	39.72	66.67
✓	✓		52.75	41.06	67.91
✓		✓	52.33	40.95	67.02
✓	✓	✓	53.00	41.13	68.41

Table 3. Ablation studies on the Refer-KITTI dataset to analyze the contribution of different modules in VMRMOT.

Method	HOTA↑	DetA↑	AssA↑
No motion feature	51.40	39.72	66.67
RoBERTa	52.46	40.74	67.70
Qwen2.5-Omni-3B	53.00	41.13	68.41

Table 4. Comparison of different methods to extract motion features on the Refer-KITTI dataset.

four NVIDIA GeForce RTX 3090 GPUs. We employ the Qwen2.5-Omni-3B [40] model as our MLLM, and all input image sequences fed into the model are resized to 336×336 . The LoRA rank is 16. The memory bank size n of \mathcal{M} is set to 4 for Refer-KITTI and 5 for Refer-KITTI-V2. The feature dimension D is 256. During inference, objects with a class confidence above 0.6 and a referring confidence above 0.4 are regarded as successfully detected objects.

4.2. Benchmark Evaluation

Refer-KITTI. We report VMRMOT’s performance on Refer-KITTI in Tab. 1. It can be seen that VMRMOT achieves the best overall performance with 53.00% HOTA, 41.13% DetA, 68.41% AssA, 26.66% MOTA, and 61.06% IDF1. Compared with other end-to-end transformer-based methods like TransRMOT [36] and TempRMOT [46], VMRMOT achieves consistent improvements, surpassing TransRMOT by 6.44% in HOTA, 3.16% in DetA, and 11.08% in AssA, and outperforming TempRMOT by 1.60%, 1.41%, and 1.74% in these metrics, respectively. These results demonstrate that the proposed vision–motion–reference alignment framework effectively enhances both detection and association performance in RMOT. In addition, it is worth noting that VMRMOT also achieves consistent improvements in the MOTA metric. Specifically, VMRMOT surpasses TransRMOT by 8.78% and TempRMOT by 1.82% in MOTA. Since MOTA is directly affected by FP and FN, this improvement provides more intuitive evidence that introducing the motion modality helps VMRMOT achieve better alignment between the reference and vision modalities.

Refer-KITTI-V2. To further validate the effectiveness of VMRMOT, we evaluate it on the Refer-KITTI-V2 dataset, which includes more linguistically diverse yet static references. As shown in Tab. 2, VMRMOT achieves the best performance with 35.21% HOTA and 23.96% DetA,

F_w^M	F_s^M	F^R	HOTA↑	DetA↑	AssA↑
✓			52.37	40.46	67.94
✓	✓		52.54	41.12	67.27
		✓	52.12	40.67	66.94
✓	✓	✓	53.00	41.13	68.41

Table 5. Comparison of different architectures of VMRA on the Refer-KITTI dataset.

F_w^M	F^R	HOTA↑	DetA↑	AssA↑
✓		52.85	41.25	67.85
	✓	51.97	40.59	66.67
✓	✓	53.00	41.13	68.41

Table 6. Comparison of different architectures of MGPB on the Refer-KITTI dataset.

as well as the second-best 51.95% AssA. Compared with TransRMOT [36] and TempRMOT [46], VMRMOT yields gains of 4.21% and 1.16% in HOTA, respectively. These results demonstrate the effectiveness of introducing the motion modality to enhance vision–reference alignment, enabling VMRMOT to maintain strong multi-modal tracking performance even under more complex references.

4.3. Ablation Studies

We conduct ablation studies on the Refer-KITTI dataset. The ablation studies focus on analyzing the contribution of different modules in VMRMOT, different methods to extract motion features, different architectures of VMRA, and different architectures of MGPB.

Contribution of Different Modules. To analyze the contribution of the proposed VMRA and MGPB modules, we conduct an ablation study, as shown in Tab. 3. In the table, “Base” refers to the baseline model without VMRA and MGPB, which corresponds to TempRMOT [46]. From the table, incorporating VMRA/MGPB achieves 52.75%/52.33% HOTA, 41.06%/40.95% DetA, and 67.91%/67.02% AssA, improving the baseline by 1.35%/0.93%, 1.34%/1.23%, and 1.24%/0.35%, respectively. The results demonstrate that incorporating the motion modality enhances vision–reference alignment, and utilizing motion cues in the prediction head further strengthens multi-modal tracking. Moreover, combining both VMRA and MGPB achieves the best performance, reaching 53.00% HOTA, 41.13% DetA, and 68.41% AssA, demonstrating that both modules contribute significantly to the overall multi-modal tracking performance of VMRMOT.

Different Methods to Extract Motion Features. To investigate the impact of different motion feature extraction methods, we conduct experiments as shown in Tab. 4. In the table, “No motion feature” denotes the baseline model without incorporating the motion modality. “RoBERTa”

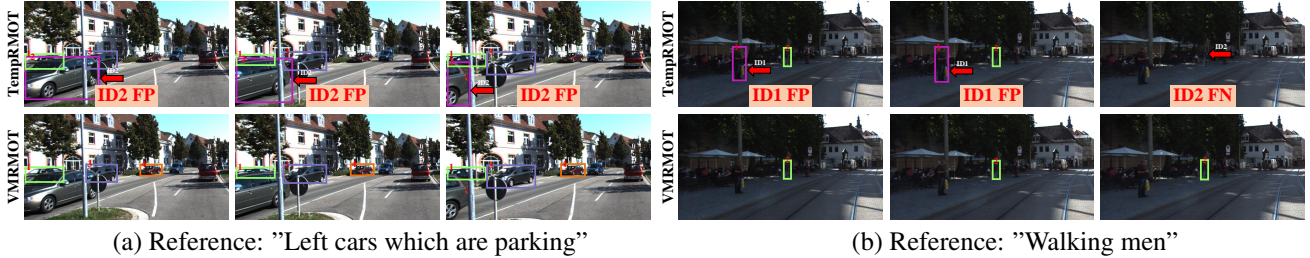


Figure 5. Qualitative comparison between TempRMOT and VMRMOT on the Refer-KITTI dataset. The red arrow indicates the noteworthy objects. Boxes of the same color represent the same ID. Best viewed in color and zoom-in.

represents extracting motion features directly from motion descriptions using a pretrained RoBERTa model. “Qwen2.5-Omni-3B” refers to extracting motion features from both motion descriptions and visual sequences using the Qwen2.5-Omni-3B model, which is used in VMRMOT. As shown in the results, the “RoBERTa” method achieves 52.46% HOTA, surpassing the baseline by 1.06%. This demonstrates that introducing a motion modality derived from motion descriptions indeed enhances cross-modal alignment and tracking performance, as the extracted motion features encode dynamic behaviors of objects. Furthermore, the “Qwen2.5-Omni-3B” method produces motion features that capture temporal correspondence between textual motion cues and visual dynamics through an MLLM, leading to the best overall tracking performance.

Different Architectures of VMRA. To evaluate the effectiveness of the VMRA architecture, we conduct experiments as shown in Tab. 5. In the table, \mathbf{F}_w^M , \mathbf{F}_s^M , and \mathbf{F}^R denote whether word-level motion features, sentence-level motion features, and reference features are incorporated into the VMRA design, respectively. As shown, integrating word-level motion features yields 52.37% HOTA, while adding sentence-level motion features further improves performance to 52.54% HOTA. When both motion and reference features are jointly fused, the model achieves the best result of 53.00% HOTA, demonstrating the effectiveness of the hierarchical fusion strategy in aligning multi-modal features. This hierarchical structure allows VMRA to capture both fine-grained motion cues and global temporal semantics, thereby enhancing multi-modal alignment and overall tracking performance. In contrast, using only reference features without motion features results in a lower 52.12% HOTA, indicating that static reference descriptions alone are insufficient for modeling temporal dynamics. The results demonstrate that incorporating motion features at multiple levels is crucial for facilitating stronger vision–reference alignment and more accurate tracking performance.

Different Architectures of MGPH. To validate the effectiveness of the MGPH design, we conduct experiments as shown in Tab. 6. In the table, \mathbf{F}_w^M and \mathbf{F}^R indicate whether motion features and reference features are incorporated in the MGPH design, respectively. As shown, incor-

porating motion features yields 52.85% HOTA, while further integrating reference features achieves the best result of 53.00% HOTA. This demonstrates that motion features effectively enhance the performance of the prediction head by providing dynamic behavioral cues of objects, and additionally, fusing reference features introduces complementary reference information that further improves prediction quality. However, when only reference features are used without motion features, the performance drops to 51.97% HOTA, indicating that reference features mainly contain static descriptions and lack dynamic cues. Therefore, the motion modality plays a more crucial role in guiding the prediction head by encoding the dynamic behaviors of objects, which are essential for accurate multi-modal tracking.

4.4. Visualization

Fig. 5 illustrates the qualitative comparison between TempRMOT [46] and VMRMOT on the Refer-KITTI dataset. As shown in Fig. 5 (a), given the RMOT reference “*Left cars which are parking*”, TempRMOT incorrectly tracks the moving object (ID2). In Fig. 5 (b), where the reference is “*walking men*”, TempRMOT incorrectly tracks the standing person (ID1) and later loses the walking person (ID2). In contrast, VMRMOT accurately tracks all referenced objects. These results demonstrate that incorporating the motion modality effectively aids in aligning the reference with the vision modality, validating the effectiveness of the proposed vision–motion–reference alignment framework for RMOT.

5. Conclusion

In this paper, we present VMRMOT, a novel vision–motion–reference alignment framework for RMOT. It introduces the motion modality to strengthen alignment between vision and reference with MLLMs. Through the proposed VMRA and MGPH, VMRMOT effectively integrates motion cues with visual–language information, achieving more robust and accurate object tracking. Extensive experiments on Refer-KITTI and Refer-KITTI-V2 demonstrate that VMRMOT consistently outperforms previous trackers, validating the effectiveness of introducing the motion modality for Referring Multi-Object Tracking.

References

- [1] Keni Bernardin and Rainer Stiefelwagen. Evaluating multiple object tracking performance: the clear mot metrics. *EURASIP Journal on Image and Video Processing*, 2008. 6
- [2] Tzoulis Chamiti, Leandro Di Bella, Adrian Munteanu, and Nikos Deligiannis. Refergpt: Towards zero-shot referring multi-object tracking. In *CVPR*, 2025. 3
- [3] Jiajun Chen, Jiacheng Lin, Guojin Zhong, You Yao, and Zhiyong Li. Multi-granularity localization transformer with collaborative understanding for referring multi-object tracking. *IEEE TIM*, 2025. 2
- [4] Jiajun Deng, Zhengyuan Yang, Tianlang Chen, Wengang Zhou, and Houqiang Li. Transvg: End-to-end visual grounding with transformers. In *ICCV*, 2021. 2
- [5] Henghui Ding, Chang Liu, Shuting He, Kaining Ying, Xudong Jiang, Chen Change Loy, and Yu-Gang Jiang. Mevis: A multi-modal dataset for referring motion expression video segmentation. *IEEE TPAMI*, 2025. 3
- [6] Yunhao Du, Cheng Lei, Zhicheng Zhao, and Fei Su. ikun: Speak to trackers without retraining. In *CVPR*, 2024. 2, 6, 12
- [7] Ruopeng Gao and Limin Wang. Memotr: Long-term memory-augmented transformer for multi-object tracking. In *ICCV*, 2023. 1
- [8] Ruopeng Gao, Ji Qi, and Limin Wang. Multiple object tracking as id prediction. In *CVPR*, 2025. 1
- [9] Andreas Geiger, Philip Lenz, and Raquel Urtasun. Are we ready for autonomous driving? the kitti vision benchmark suite. In *CVPR*. IEEE, 2012. 6
- [10] Wenyan He, Yajun Jian, Yang Lu, and Hanzi Wang. Visual-linguistic representation learning with deep cross-modality fusion for referring multi-object tracking. In *ICASSP*. IEEE, 2024. 2, 6
- [11] Edward J Hu, Yelong Shen, Phillip Wallis, Zeyuan Allen-Zhu, Yuanzhi Li, Shean Wang, Lu Wang, Weizhu Chen, et al. Lora: Low-rank adaptation of large language models. *ICLR*, 2022. 6, 11
- [12] Bingliang Jiao, Lingqiao Liu, Liying Gao, Ruiqi Wu, Guosheng Lin, Peng Wang, and Yanning Zhang. Toward re-identifying any animal. *NeurIPS*, 2023. 2
- [13] Bahjat Kawar, Shiran Zada, Oran Lang, Omer Tov, Huiwen Chang, Tali Dekel, Inbar Mosseri, and Michal Irani. Magic: Text-based real image editing with diffusion models. In *CVPR*, 2023. 2
- [14] Dezhuang Li, Ruoqi Li, Lijun Wang, Yifan Wang, Jinqing Qi, Lu Zhang, Ting Liu, Qingquan Xu, and Huchuan Lu. You only infer once: Cross-modal meta-transfer for referring video object segmentation. In *AAAI*, 2022. 2
- [15] Guorong Li, Hanhua Ye, Yuankai Qi, Shuhui Wang, Laiyun Qing, Qingming Huang, and Ming-Hsuan Yang. Learning hierarchical modular networks for video captioning. *IEEE TPAMI*, 2023. 2
- [16] Guangyao Li, Siping Zhuang, Yajun Jian, Yan Yan, and Hanzi Wang. Language decoupling with fine-grained knowledge guidance for referring multi-object tracking. In *ICCV*, 2025. 2, 3
- [17] Xiang Li, Jinglu Wang, Xiaohao Xu, Xiao Li, Bhiksha Raj, and Yan Lu. Robust referring video object segmentation with cyclic structural consensus. In *ICCV*, 2023. 2
- [18] Yizhe Li, Sanping Zhou, Zheng Qin, and Le Wang. Visual-linguistic feature alignment with semantic and kinematic guidance for referring multi-object tracking. *IEEE TMM*, 2025. 2, 3
- [19] Chao Liang, Zhipeng Zhang, Xue Zhou, Bing Li, Shuyuan Zhu, and Weiming Hu. Rethinking the competition between detection and reid in multiobject tracking. *IEEE TIP*, 2022. 6
- [20] Shaofeng Liang, Runwei Guan, Wangwang Lian, Daizong Liu, Xiaolou Sun, Dongming Wu, Yutao Yue, Weiping Ding, and Hui Xiong. Cognitive disentanglement for referring multi-object tracking. *Information Fusion*, 2025. 2, 3
- [21] Tianming Liang, Kun-Yu Lin, Chaolei Tan, Jianguo Zhang, Wei-Shi Zheng, and Jian-Fang Hu. Referdino: Referring video object segmentation with visual grounding foundations. *arXiv preprint arXiv:2501.14607*, 2025. 2
- [22] Guibiao Liao, Jiankun Li, and Xiaoqing Ye. Vlm2scene: Self-supervised image-text-lidar learning with foundation models for autonomous driving scene understanding. In *AAAI*, 2024. 2
- [23] Jiacheng Lin, Jiajun Chen, Kunyu Peng, Xuan He, Zhiyong Li, Rainer Stiefelwagen, and Kailun Yang. Echotrack: Auditory referring multi-object tracking for autonomous driving. *IEEE TITS*, 2024. 6
- [24] Tsung-Yi Lin, Priya Goyal, Ross Girshick, Kaiming He, and Piotr Dollár. Focal loss for dense object detection. In *ICCV*, 2017. 11
- [25] Yinhan Liu, Myle Ott, Naman Goyal, Jingfei Du, Mandar Joshi, Danqi Chen, Omer Levy, Mike Lewis, Luke Zettlemoyer, and Veselin Stoyanov. Roberta: A robustly optimized bert pretraining approach. *arXiv preprint arXiv:1907.11692*, 2019. 3
- [26] Jonathon Luiten, Aljosa Osep, Patrick Dendorfer, Philip Torr, Andreas Geiger, Laura Leal-Taixé, and Bastian Leibe. Hota: A higher order metric for evaluating multi-object tracking. *IJCV*, 2021. 6
- [27] Weiyi Lv, Ning Zhang, Junjie Zhang, and Dan Zeng. One-shot multiple object tracking with robust id preservation. *IEEE TCSVT*, 2023. 1
- [28] Weiyi Lv, Yuhang Huang, Ning Zhang, Rwei-Sung Lin, Mei Han, and Dan Zeng. Diffmot: A real-time diffusion-based multiple object tracker with non-linear prediction. In *CVPR*, 2024. 1
- [29] Zeliang Ma, Song Yang, Zhe Cui, Zhicheng Zhao, Fei Su, Delong Liu, and Jingyu Wang. Mls-track: Multilevel semantic interaction in rmot. *arXiv preprint arXiv:2404.12031*, 2024. 2
- [30] Tim Meinhardt, Alexander Kirillov, Laura Leal-Taixé, and Christoph Feichtenhofer. Trackformer: Multi-object tracking with transformers. In *CVPR*, 2022. 6
- [31] Ergys Ristani, Francesco Solera, Roger Zou, Rita Cucchiara, and Carlo Tomasi. Performance measures and a data set for multi-target, multi-camera tracking. In *ECCV*. Springer, 2016. 6

- [32] Seonguk Seo, Joon-Young Lee, and Bohyung Han. Urvos: Unified referring video object segmentation network with a large-scale benchmark. In *ECCV*. Springer, 2020. 2
- [33] Nicholas Stroh. Trackgpt—a generative pre-trained transformer for cross-domain entity trajectory forecasting. *arXiv preprint arXiv:2402.00066*, 2024. 3
- [34] Peize Sun, Jinkun Cao, Yi Jiang, Rufeng Zhang, Enze Xie, Zehuan Yuan, Changhu Wang, and Ping Luo. Transtrack: Multiple object tracking with transformer. *arXiv preprint arXiv:2012.15460*, 2020. 6
- [35] Nicolai Wojke, Alex Bewley, and Dietrich Paulus. Simple online and realtime tracking with a deep association metric. In *ICIP*. IEEE, 2017. 6
- [36] Dongming Wu, Wencheng Han, Tiancai Wang, Xingping Dong, Xiangyu Zhang, and Jianbing Shen. Referring multi-object tracking. In *CVPR*, 2023. 2, 3, 6, 7, 12
- [37] Dongming Wu, Tiancai Wang, Yuang Zhang, Xiangyu Zhang, and Jianbing Shen. Onlinerefer: A simple online baseline for referring video object segmentation. In *ICCV*, 2023. 2
- [38] Jiannan Wu, Yi Jiang, Peize Sun, Zehuan Yuan, and Ping Luo. Language as queries for referring video object segmentation. In *CVPR*, 2022. 2
- [39] Changcheng Xiao, Qiong Cao, Yujie Zhong, Xiang Zhang, Tao Wang, Canqun Yang, and Long Lan. Temporal-enhanced multimodal transformer for referring multi-object tracking and segmentation. *IEEE TCSVT*, 2025. 2
- [40] Jin Xu, Zhifang Guo, Jinzheng He, Hangrui Hu, Ting He, Shuai Bai, et al. Qwen2.5-omni technical report. *arXiv preprint arXiv:2503.20215*, 2025. 7, 11
- [41] Cilin Yan, Haochen Wang, Shilin Yan, Xiaolong Jiang, Yao Hu, Guoliang Kang, Weidi Xie, and Efstratios Gavves. Visa: Reasoning video object segmentation via large language models. In *ECCV*. Springer, 2024. 3
- [42] Fangao Zeng, Bin Dong, Yuang Zhang, Tiancai Wang, Xiangyu Zhang, and Yichen Wei. Motr: End-to-end multiple-object tracking with transformer. In *ECCV*. Springer, 2022. 2, 3
- [43] Yifu Zhang, Chunyu Wang, Xinggang Wang, Wenjun Zeng, and Wenyu Liu. Fairmot: On the fairness of detection and re-identification in multiple object tracking. *IJCV*, 2021. 6, 12
- [44] Yifu Zhang, Peize Sun, Yi Jiang, Dongdong Yu, Fucheng Weng, Zehuan Yuan, Ping Luo, Wenyu Liu, and Xinggang Wang. Bytetrack: Multi-object tracking by associating every detection box. In *ECCV*. Springer, 2022. 1, 6, 12
- [45] Yujia Zhang, Qianzhong Li, Yi Pan, Xiaoguang Zhao, and Min Tan. Multi-stage image-language cross-generative fusion network for video-based referring expression comprehension. *IEEE TIP*, 2024. 2
- [46] Yani Zhang, Dongming Wu, Wencheng Han, and Xingping Dong. Bootstrapping referring multi-object tracking. *arXiv preprint arXiv:2406.05039*, 2024. 2, 5, 6, 7, 8, 12, 14, 15
- [47] Lichen Zhao, Daigang Cai, Lu Sheng, and Dong Xu. 3dvg-transformer: Relation modeling for visual grounding on point clouds. In *ICCV*, 2021. 2
- [48] Rongkun Zheng, Lu Qi, Xi Chen, Yi Wang, Kun Wang, and Hengshuang Zhao. Villa: Video reasoning segmentation with large language model. In *ICCV*, 2025. 3
- [49] Li Zhou, Zikun Zhou, Kaige Mao, and Zhenyu He. Joint visual grounding and tracking with natural language specification. In *CVPR*, 2023. 2
- [50] Siping Zhuang, Guangyao Li, Qiangqiang Wu, Yang Lu, Hai-Miao Hu, and Hanzi Wang. Cgatracker: Correlation-aware graph alignment for referring multi-object tracking. *IEEE TCSVT*, 2025. 2

Vision–Motion–Reference Alignment for Referring Multi-Object Tracking via Multi-Modal Large Language Models

Supplementary Material

A. More MLLM and Fine-tuning Details

In our framework, we adopt Qwen2.5-Omni-3B [40] as the MLLM for motion feature extraction. Due to its compact yet expressive multi-modal design supporting both textual and video inputs, the model is well suited for RMOT. It enables joint encoding of linguistic cues and frame-level visual content, facilitating effective alignment in video-based tracking. In practice, we utilize the *Thinker* component of Qwen2.5-Omni-3B to encode the motion-aware descriptions together with the corresponding visual sequence consisting of the previous n frames. The Thinker module is designed for multi-modal fusion and reasoning, and the representations produced at its final layer have undergone multiple rounds of cross-modal interaction. Therefore, we use the last-layer hidden states as motion features.

A.1. Input and Feature Extraction

As described in the main paper, for each tracked object at frame f , we construct a motion-aware textual description \mathcal{E}_f^M and provide the previous n visual frames $\mathcal{V}_f^{hist} = \{\mathbf{F}_{f-n}^{vis}, \dots, \mathbf{F}_f^{vis}\}$ as multi-modal input. Then, both \mathcal{E}_f^M and \mathcal{V}_f^{hist} are fed into the *Thinker* component of Qwen2.5-Omni-3B, which performs joint cross-modal encoding and produces hidden representations at each transformer layer.

Let $\text{MLLM}_{\text{thinker}}(\cdot)$ denote this module. We use the hidden states from the last layer as our word-level motion representation:

$$F_w^M = \text{MLLM}_{\text{thinker}}(\mathcal{E}_f^M, \mathcal{V}_f^{hist}) \in \mathbb{R}^{L^M \times D^M}, \quad (11)$$

where D^M is the hidden dimension of the MLLM. A mask-weighted average is applied to obtain the sentence-level motion feature:

$$F_s^M = \frac{\sum_{l=1}^{L^M} m_l F_{w,l}^M}{\sum_{l=1}^{L^M} m_l}, \quad (12)$$

where m_l denotes the attention mask for token l .

A.2. Feature Projection

To align the MLLM features with the tracking queries, we employ a learnable linear layer:

$$F_s^M = \text{Linear}(F_s^M), \quad (13)$$

which maps the motion feature into the transformer embedding space D used in VMRMOT.

A.3. LoRA-based Fine-tuning

Although Qwen2.5-Omni-3B is pretrained on large-scale multi-modal data, its text encoder and fusion modules are not naturally optimized for the motion-aware descriptions used in our setting. Therefore, we finetune the MLLM in a parameter-efficient manner using LoRA [11].

Concretely, we apply LoRA to the last N_{layer} layers of the text encoder as well as the fusion modules within the Thinker component. The low-rank adaptation is injected into both the self-attention and feed-forward sublayers. This strategy allows the MLLM to adapt to domain-specific motion descriptions while keeping most parameters frozen, resulting in high efficiency with minimal computational overhead.

B. Training Loss

VMRMOT is supervised through three branches: a class branch, a box regression branch, and a referring branch. The box branch is supervised using an L1 loss together with a Generalized IoU (GIoU) loss, while both the class and referring branches are supervised using the focal loss [24].

Box Regression Branch. The box regression branch predicts normalized bounding boxes \hat{b} for each query. It is supervised by a combination of L1 loss and the GIoU loss:

$$\mathcal{L}_{\text{box}} = \|\hat{b} - b\|_1 + (1 - \text{GIoU}(\hat{b}, b)), \quad (14)$$

where b denotes the ground-truth box. The L1 loss encourages precise coordinate regression, while GIoU provides a more robust geometric overlap measure.

Class and Referring Branches. Both the class branch and the referring branch produce probability outputs \hat{p} over their respective label spaces. They are supervised using the focal loss:

$$\mathcal{L}_{\text{focal}} = -\alpha_t (1 - p_t)^\gamma \log(p_t), \quad (15)$$

where p_t is the predicted probability corresponding to the ground-truth class, α is a class-balancing factor, and γ is a factor to control the focusing strength. The focal loss mitigates label imbalance and encourages the model to focus on harder samples.

Overall Loss. The overall training loss is formulated as a weighted sum of the three branches:

$$\mathcal{L} = \lambda_{\text{class}} \mathcal{L}_{\text{class}} + \lambda_{\text{ref}} \mathcal{L}_{\text{ref}} + \lambda_{\text{box}} \mathcal{L}_{\text{box}}. \quad (16)$$

Here, λ_{class} , λ_{ref} , and λ_{box} serve as weighting factors for $\mathcal{L}_{\text{class}}$, \mathcal{L}_{ref} , and \mathcal{L}_{box} , respectively.

Method	E	HOTA \uparrow	DetA \uparrow	AssA \uparrow	IDF1 \uparrow
FairMOT [43]	✗	22.53	15.80	32.82	-
ByteTrack [44]	✗	24.59	16.78	36.63	-
iKUN [6]	✗	10.32	2.17	49.77	-
TransRMOT [36]	✓	31.00	19.40	49.68	-
TempRMOT \ddagger [46]	✓	34.05	22.22	52.50	35.71
VMRMOT	✓	35.21	23.96	51.95	37.14

Table 7. Comparison with state-of-the-art RMOT trackers on the Refer-KITTI-V2 test sets. \ddagger represents the results obtained by directly evaluating using the official open source code and weights. "E" means the End-to-End methods. \uparrow means the higher the better. **Bold** numbers indicate the best results.

C. More Analysis on Refer-KITTI-V2 Results

As reported in the main paper and summarized in Tab. 7 (corresponding to Tab. 2 in the main paper), VMRMOT consistently achieves the highest HOTA and DetA on the Refer-KITTI-V2 dataset, surpassing both TransRMOT [36] and TempRMOT [46]. It also obtains the second-best AssA among all compared methods. In addition, we further report the IDF1 metric in this supplement, where VMRMOT obtains the best IDF1 of 37.14%, outperforming TempRMOT by 1.43%. These results demonstrate that incorporating the motion modality effectively strengthens vision-reference alignment, enabling more robust tracking under challenging static and linguistically diverse references.

Although VMRMOT exhibits a slightly lower AssA compared to TempRMOT, its higher IDF1 indicates stronger identity consistency throughout the tracking process. AssA measures identity association conditioned on correct detections. On Refer-KITTI-V2, the complex and diverse descriptions make precise bounding-box localization more challenging; even small localization fluctuations or brief motion ambiguities can reduce the association score. TempRMOT places stronger emphasis on temporal smoothness, leading to slightly steadier short-term localization and thus a marginally higher AssA. In contrast, VMRMOT focuses on introducing the motion modality to enhance vision-reference alignment and improve multi-modal tracking. This design yields higher IDF1 and HOTA, which more comprehensively reflect the advantages of VMRMOT under challenging and diverse references.

Overall, the results indicate that VMRMOT demonstrates stronger identity preservation, as reflected by its highest IDF1 score, while maintaining competitive association accuracy (AssA) and achieving state-of-the-art HOTA and DetA.

D. Details of Motion-aware Description Generation

In the main paper, we introduce four descriptors (position, motion direction, distance trend, and speed trend) to characterize the dynamic behaviors of tracked objects. Here, we provide the complete deterministic rule set that converts the historical motion information $I = \{B_{f-n}, B_{f-n+1}, \dots, B_f\}$, where $B_f = (x_f, y_f, w_f, h_f)$ denotes the bounding box at frame f , into the textual motion-aware description \mathcal{E}^M .

D.1. Position Descriptor

Using normalized center coordinates (as in Eq. 1 of the main paper) $P_f = (\frac{x_f}{W}, \frac{y_f}{H})$, define offsets

$$d_x = \frac{x_f}{W} - 0.5, \quad d_y = \frac{y_f}{H} - 0.5. \quad (17)$$

We define the position descriptor $pos \equiv \langle position\ descriptor \rangle$ as:

$$pos = \begin{cases} \text{"in front"}, & |d_x| < 0.05, |d_y| < 0.05, \\ \text{"ahead"}, & d_y < -0.05, |d_x| < 0.1, \\ \text{"behind"}, & d_y > 0.05, |d_x| < 0.1, \\ \text{"on the left"}, & d_x < -0.05, |d_y| < 0.1, \\ \text{"on the right"}, & d_x > 0.05, |d_y| < 0.1, \\ \text{"front-left"}, & d_y < -0.05, d_x < -0.05, \\ \text{"front-right"}, & d_y < -0.05, d_x > 0.05, \\ \text{"back-left"}, & d_y > 0.05, d_x < -0.05, \\ \text{"back-right"}, & d_y > 0.05, d_x > 0.05, \\ \text{"in front"}, & \text{otherwise.} \end{cases} \quad (18)$$

The position descriptor captures the object's relative location in the frame. By normalizing the bounding box center coordinates and comparing them to the image center, we categorize the object into spatial regions. This provides a coarse yet interpretable spatial context for motion reasoning.

D.2. Motion Direction Descriptor

Define displacement between consecutive frames (matches Eq. 2 in the main paper):

$$\Delta x_f = x_f - x_{f-1}, \quad \Delta y_f = y_f - y_{f-1}. \quad (19)$$

We define the motion direction descriptor $md \equiv \langle \text{motion direction} \rangle$ as:

$$md = \begin{cases} \text{“moving forward”}, & \Delta y_f < -\tau_y, \\ \text{“moving backward”}, & \Delta y_f > \tau_y, \\ \text{“moving left”}, & |\Delta y_f| \leq \tau_y, \Delta x_f < -\tau_x, \\ \text{“moving right”}, & |\Delta y_f| \leq \tau_y, \Delta x_f > \tau_x, \\ \text{“motion unclear”}, & \text{otherwise,} \end{cases} \quad (20)$$

where $\tau_x = 0.005$ and $\tau_y = 0.001$. If longitudinal motion is present ($|\Delta y_f| > \tau_y$) and lateral displacement exceeds τ_x , append a lateral description:

$$md = \begin{cases} md + \text{“slightly left”}, & |\Delta y_f| > \tau_y, \Delta x_f < -\tau_x, \\ md + \text{“slightly right”}, & |\Delta y_f| > \tau_y, \Delta x_f > \tau_x, \\ md, & \text{otherwise.} \end{cases} \quad (21)$$

The motion direction descriptor captures the orientation of the object’s movement between consecutive frames. By analyzing the displacement $(\Delta x_f, \Delta y_f)$, we determine whether the object is moving forward, backward, left, or right. If both longitudinal and lateral displacements are significant, a “slightly left/right” modifier is appended. This design prioritizes forward/backward motion while providing finer-grained lateral adjustments.

D.3. Distance Trend Descriptor

Let the area $A_t = w_t \cdot h_t$. Define area change $\Delta A_f = A_f - A_{f-1}$ (matches Eq. 3 in the main paper). We define the distance trend descriptor $dt \equiv \langle \text{distance trend} \rangle$ as:

$$dt = \begin{cases} \text{“approaching”}, & A_f > A_{f-1}(1 + \epsilon), \\ \text{“moving away”}, & A_f < A_{f-1}(1 - \epsilon), \\ \text{“keeping distance”}, & \text{otherwise,} \end{cases} \quad (22)$$

where $\epsilon = 0.05$. The distance trend descriptor captures the object’s relative motion along the depth direction in the image. An increase in bounding box area indicates approaching, a decrease indicates moving away, and a negligible change indicates keeping distance. The threshold ϵ mitigates minor fluctuations in box sizes, ensuring robustness against detection noise.

D.4. Speed Trend Descriptor

Compute speed and speed change (matches Eq. 4 in the main paper):

$$v_f = \sqrt{(\Delta x_f)^2 + (\Delta y_f)^2}, \quad \Delta v_f = v_f - v_{f-1}. \quad (23)$$

Motion Representation	HOTA↑	DetA↑	AssA↑
Numeric	52.34	40.72	67.42
Descriptive	53.00	41.13	68.41

Table 8. Comparison of different motion representations on the Refer-KITTI dataset. “Numeric” encodes motion as numerical vectors via a Transformer, while “Descriptive” converts motion into natural-language descriptions processed by the MLLM. The best results are shown in bold.

The speed trend descriptor $st \equiv \langle \text{speed trend} \rangle$ is:

$$st = \begin{cases} \text{“accelerating”}, & \Delta v_f > \delta, \\ \text{“decelerating”}, & \Delta v_f < -\delta, \\ \text{“constant speed”}, & |\Delta v_f| \leq \delta, \end{cases} \quad (24)$$

where $\delta = 0.001$. The speed trend descriptor captures changes in the magnitude of object velocity, reflecting acceleration or deceleration. By computing the speed difference Δv_f over consecutive frames, we identify whether the object is accelerating, decelerating, or moving at a constant speed.

D.5. Frame-level output rules

Let N_{valid} be the number of valid (non-zero) frames in the retrieved history.

$$\mathcal{E}^M = \begin{cases} \text{Target is } \langle \text{position} \rangle, & N_{\text{valid}} = 1, \\ \text{Target is } \langle \text{position} \rangle, \\ \langle \text{motion direction} \rangle, \\ \langle \text{distance trend} \rangle & , N_{\text{valid}} = 2, \\ \text{Target is } \langle \text{position} \rangle, \\ \langle \text{motion direction} \rangle, \\ \langle \text{distance trend} \rangle \text{ and} \\ \langle \text{speed trend} \rangle & , N_{\text{valid}} \geq 3, \end{cases} \quad (25)$$

Here, the frame-level output \mathcal{E}^M adapts to the number of valid frames N_{valid} in the retrieved history. When $N_{\text{valid}} = 1$, the description includes only the position descriptor. When $N_{\text{valid}} = 2$, the description contains the position, motion direction, and distance trend descriptors. When $N_{\text{valid}} \geq 3$, all four descriptors, including speed trend, are included.

E. More Experiments

Impact of Motion Representation Form. We evaluate how different formulations of motion information affect tracking performance. As shown in Tab. 8, representing motion as numeric vectors and encoding them with a Transformer yields 52.34% HOTA. This approach provides only

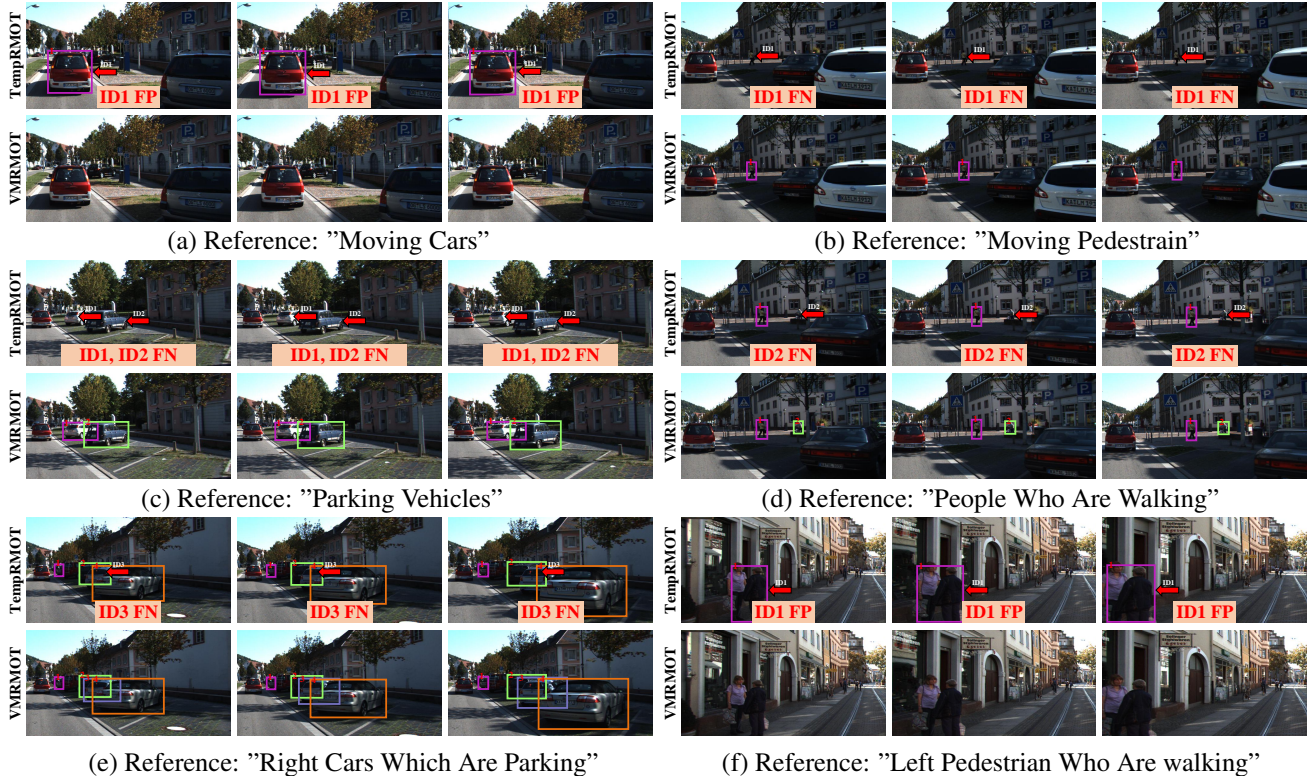


Figure 6. Qualitative comparison between TempRMOT and VMRMOT on the Refer-KITTI dataset. The red arrow indicates the noteworthy objects. Boxes of the same color represent the same ID. Best viewed in color and zoom-in.

N_{layer}	HOTA \uparrow	DetA \uparrow	AssA \uparrow
4	51.54	39.96	66.61
8	53.00	41.13	68.41
16	49.66	37.99	65.04
32	50.15	38.46	65.51

Table 9. Evaluation of the number of fine-tuning layers N_{layer} on the Refer-KITTI dataset. The best results are shown in bold.

moderate improvements because raw numerical inputs lack sufficient semantic expressiveness. In contrast, converting motion into natural-language descriptions and encoding them with the MLLM leads to a clear performance gain, achieving 53.00% HOTA. This improvement suggests that descriptive motion language provides richer temporal and semantic cues, allowing the MLLM to better align motion information with visual evidence and thus enhance multi-modal tracking.

The Number of Fine-tuning Layers N_{layer} . We conduct an ablation study to investigate how many of the last layers of the MLLM text encoder should be finetuned. As shown in Tab. 9, fine-tuning only the last 4 layers yields

51.54% HOTA, and the model still lacks sufficient capacity to fully adapt to motion-aware descriptions. Increasing the number of trainable layers to 16 or 32 leads to performance drops (49.66% and 50.15% HOTA, respectively), as excessive fine-tuning disrupts deeper linguistic representations and introduces instability in cross-modal alignment. Fine-tuning the last 8 layers achieves the best performance with 53.00% HOTA. This setting provides a good balance between adaptability and stability, enabling the model to learn motion-specific semantics while preserving its pre-trained language understanding capability.

F. More Visualization

F.1. Qualitative Comparison on Refer-KITTI

Fig. 6 illustrates additional qualitative comparisons between TempRMOT [46] and our VMRMOT on the Refer-KITTI dataset. As shown, TempRMOT frequently suffers from a large number of FPs and FNs due to the temporal discrepancy between the visual modality and the static references. For example, the issue happens on the tracking results by TempRMOT at: (a) ID1 FP; (b) ID1 FN; (c) ID1 FN and ID2 FN; (d) ID2 FN; (e) ID3 FN; (f) ID1 FP. In contrast, VMRMOT achieves accurate tracking throughout the entire sequence. By introducing the motion modality, VMRMOT



Figure 7. Qualitative comparison between TempRMOT and VMRMOT on the Refer-KITTI-V2 dataset. The red arrow indicates the noteworthy objects. Boxes of the same color represent the same ID. Best viewed in color and zoom-in.

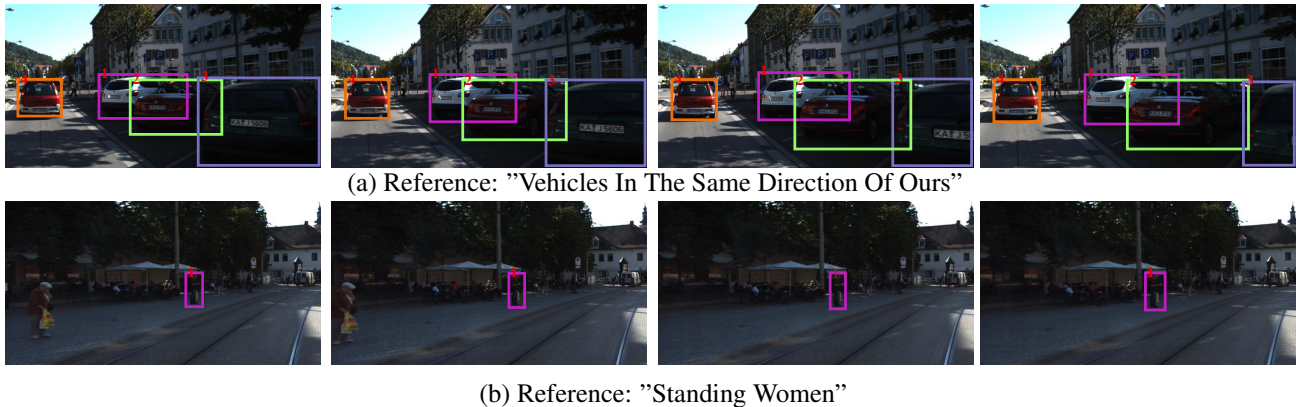


Figure 8. Illustration of two failure cases. We show the two failure cases of our approach. Boxes of the same color represent the same ID. Best viewed in color and zoom-in.

effectively bridges the temporal discrepancy between the visual modality and references, enabling robust multi-modal tracking.

F.2. Qualitative Comparison on Refer-KITTI-V2

Fig. 7 illustrates the qualitative comparison between TempRMOT [46] and VMRMOT on the Refer-KITTI-V2 dataset. Due to the increased linguistic diversity and com-

plexity of the static references in Refer-KITTI-V2, TempRMOT exhibits numerous FP and FN cases, further amplifying the temporal discrepancy between the visual modality and the static references. For instance, TempRMOT produces erroneous tracking results in: (a) ID1 FN; (b) ID1 FP; (c) ID1 FP; (d) ID1 FP and ID2 FP; (e) ID1 FP; (f) ID1 FP. In contrast, VMRMOT yields more accurate

and stable tracking results throughout the sequence. By leveraging the motion modality, VMRMOT effectively mitigates the temporal discrepancy and achieves more reliable vision–reference alignment, even under more diverse and challenging references.

G. Illustration of Failure Cases

We visualize two failure cases in Fig. 8. In the first case, with the reference expression “*vehicles in the same direction of ours*”, VMRMOT incorrectly tracks parked vehicles on the right side (ID1, ID2, and ID3). In the second case, given the reference “*standing women*”, the tracker mistakenly tracks a standing man (ID1). These errors mainly occur because the reference is still encoded purely by a text encoder, without jointly incorporating visual context during reference understanding. As a result, the model lacks fine-grained scene grounding ability and may misinterpret semantic categories or contextual constraints. We believe that adopting a multi-modal encoding strategy, where both the reference and the visual scene are jointly modeled, could enhance semantic grounding and reduce such errors, ultimately improving tracking accuracy in complex real-world scenarios.